loss is measured using an Agilent HP 8719ES Vector Network Analyzer (VNA). Figures 9(a) and 9(b) show the top side and the bottom side, respectively, of the novel antenna on the dielectric substrate.

The measured and simulated results of return losses for the proposed antenna are shown in Figure 10. The ultra-wideband behavior is confirmed by the measured and an acceptable agreement between measurement and simulation is observed. This difference is due to the measurement conditions. The proposed antenna can achieve a bandwidth from 2.9 to 10.8 GHz (115.32%).

5. CONCLUSION

This article has proposed a novel printed monopole antenna with modified notched semi-elliptical ground plane. The dependence of the bandwidth on the main parameters has been investigated. The proposed antenna has an omnidirectional pattern at *x-y* plane for all the measured impedance bandwidth (2.9−10.8 GHz), which covers the commercial UWB band. It shows that there is an acceptable agreement between the measured results, and the simulated ones for the entire operating band.

REFERENCES

1. FCC, First report and order on ultra-wideband technology, Washington, DC, 2002.
2. E. A-Daviu, M.C. Fabres, M.F. Bataller, and A.V. Nogueira, Wideband double-fed planar monopole antennas, Electron Lett 39 (2003), 1635–1636.
3. M.J. Ammann and Z.N. Chen, Wideband monopole antennas for multi-band wireless systems, IEEE Antennas Propag Mag 45 (2003), 146–150.
4. W. Wang, S.S. Zhong, and S.B. Chen, A novel wideband coplanar-fed monopole antenna, Microwave Opt Technol Lett 43 (2004), 50–52.
5. M.J. Ammann and Z.N. Chen, An asymmetrical feed arrangement for improved impedance bandwidth of planar monopole antennas, Microwave Opt Technol Lett 40 (2004), 156–158.
6. M. John and M.J. Ammann, Optimisation of impedance bandwidth for the printed rectangular monopole antenna, Microwave Opt Technol Lett (2005), 153–154.
7. C. Zhang and A.E. Fathy, Development of an ultra-wideband elliptical disc planar monopole antenna with improved omni-directional performance using a modified ground, IEEE Antennas and Propagation Symposium Digest, Alburqueque, NM, 2006, pp. 1689–1692.
8. C.-Y. Huang and W.-C. Hsia, Planar elliptical antenna for ultra-wideband communications, Electron Lett 41 (2005), 296–297.
9. X.L. Bao and M.J. Ammann, Investigation on UWB printed monopole antenna with rectangular slitted ground plane, Microwave Opt Technol Lett 49 (2007), 1585–1587.
10. H. Kobayashi, T. Sasamori, T. Tobana, and K. Abe, A study on miniaturization of printed disc monopole antenna for UWB applications using notched ground plane, IEICE Trans Commun 90 (2007), 2239–2245.

ISOLATION IMPROVEMENT OF 2.4/5.2/5.8 GHz WLAN INTERNAL LAPTOP COMPUTER ANTENNAS USING DUAL-BAND STRIP RESONATOR AS A WAVETRAP

Ting-Wei Kang and Kin-Lu Wong
Department of Electrical Engineering, National Sun Yat-Sen University, Kaohsiung 804, Taiwan; Corresponding author: wongkl@ema.ee.nsysu.edu.tw

Received 20 April 2009

ABSTRACT: *A high-isolation two-antenna structure comprising two small-size uniplanar WLAN antennas and a dual-band strip resonator embedded in-between for laptop computer application is presented. The proposed design occupies a small planar size of 9 × 50 mm^2 when mounted above the top edge of the large supporting metal frame of the laptop display. The two WLAN antennas are coupled-fed printed PIFAs capable of covering 2.4/5.2/5.8 GHz band operation, each occupying a size of 9 × 13 mm^2 and both facing to each other back-to-back with a spacing of 24 mm (that is, the total length of the proposed two-antenna structure is 50 mm). The embedded strip resonator functions as a dual-band wavetrap over the 2.4 and 5.2/5.8 GHz bands to trap the antenna's near-field radiation between the two antennas, which effectively reduces the mutual coupling between the two antennas. Good measured isolation ($S_{21} < -18$ dB) over the 2.4/5.2/5.8 GHz bands is obtained, which is acceptable for practical laptop computer applications. The proposed design works for the large ground plane condition in the laptop computer, different from many of the reported two-antenna designs working for the relatively much smaller ground plane conditions such as in the mobile phones and PC cards.* © 2009 Wiley Periodicals, Inc. Microwave Opt Technol Lett 52: 58–64, 2010; Published online in Wiley InterScience (www.interscience.wiley.com). DOI 10.1002/mop.24831

Key words: *internal laptop computer antenna; WLAN antenna; isolation improvement; printed antenna; dual-band strip resonator*

1. INTRODUCTION

A variety of promising internal 2.4/5.2/5.8 GHz WLAN (wireless local area network) antennas suitable for application in the laptop computer such as the notebook and netbook [1] have been reported in the published articles [2–11]. Among the reported internal WLAN laptop computer antennas, the traditional designs use the metal-plate PIFA (planar inverted-F antenna) elements [2–4] and many recent designs apply the planar printed antenna elements [5–10]. For the recent designs, it has been shown that by using the coupling feed, the printed PIFA or shorted monopole antenna can easily cover 2.4/5.2/5.8 GHz WLAN bands (2400–2484/5150–5350/5725–5875 MHz) with a small size. The antenna length along the top edge of the large supporting metal frame of the laptop display can be generally less than about 13 mm [7–10], which is much smaller than that of the traditional designs using the metal-plate PIFA elements (antenna length usually larger than 35 mm) [2–4]. The antenna size reduction is obtained mainly because the lowest or fundamental resonant mode of the PIFA or shorted monopole antenna can be successfully excited at frequencies less than those of the traditional quarter-wavelength resonant mode. This behavior is made possible owing to the introduced coupling feed contributing additional capacitance to compensate for the large inductive reactance caused by the decreased resonant length of the PIFA or shorted monopole antenna [7–10, 12].

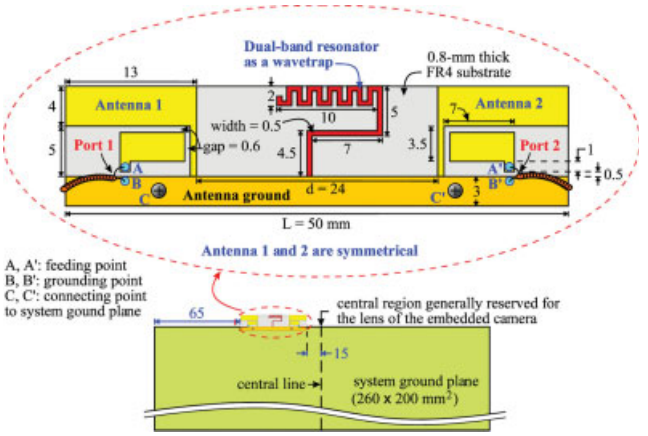

Figure 1 Geometry of two 2.4/5.2/5.8 GHz WLAN internal laptop computer antennas using a dual-band strip resonator as a wavetrap for isolation improvement. [Color figure can be viewed in the online issue, which is available at www.interscience.wiley.com]

Owing to their planar structure showing thin thickness (generally less than 1 mm), these printed coupled-fed PIFAs [7–10] are attractive for application as internal WLAN antennas in the modern thin-profile laptop computer [13–15]. However, for practical applications in the laptop computer, at least two WLAN antennas with reduced mutual coupling are usually demanded to enhance the signal transmission and reception such as in the MIMO (multiple input multiple output) operation [16–20]. For such applications, a two-antenna structure occupying a small area and having reduced mutual coupling is demanded. Although there have been related studies on the two-antenna structure for performing 2.4/5.2/5.8 GHz WLAN operation [16–21], they are mainly working for small ground plane conditions such as about the size of 50 × 90 mm^2 in the mobile phones, PC cards, and so on. Because the small ground plane can be a part of the radiator, a certain portion of the excited surface currents on the ground plane can be directed in the direction orthogonal to that of the two antennas along the top edge of the ground plane. This condition can effectively result in decreased mutual coupling between the two antennas. Hence, it has been shown that by placing two WLAN PIFAs with their shorting arms facing to each other, good isolation between the two antennas can be obtained with a small spacing of 5 mm between the two antennas [21].

For the large ground plane condition (size 200 × 260 mm^2 studied here) in the laptop computer, it becomes a different scenario. The ground plane is no longer a part of an effective radiator, and hence much stronger antenna radiation is directed to each other for the two antennas. In this case, an increased spacing between the two antennas is required for achieving acceptable mutual coupling of the two antennas for practical applications such as in the MIMO operation. Although embedding resonant slits in the ground plane [18, 19] can be a good method to lengthen the effective spacing between the two antennas along the top edge of the ground plane, it is usually not attractive because it may require the redesign of the circuit layout on the ground plane to accommodate the embedded slits and some undesired EMC (electromagnetic compatibility) issues may also occur.

In this article, we present a two-antenna structure comprising two small-size uniplanar WLAN antennas and a dual-band strip resonator embedded in-between to achieve enhanced isolation for laptop computer application. The dual-band strip resonator can function like a wavetrap over the 2.4 and 5.2/5.8 GHz bands to effectively reduce the mutual coupling between the two antennas through trapping or blocking the antenna's near-field radiation. With the proposed design, good measured isolation ($S_{21} < -18$ dB) over the 2.4/5.2/5.8 GHz bands for the two antennas with a small spacing of 24 mm is obtained, and the total length of the proposed design including the two 2.4/5.2/5.8 GHz WLAN antennas is 50 mm only, generally acceptable for practical laptop computer applications. With the reduced mutual coupling, good decorrelated radiation patterns for the two antennas can be obtained, which is important for MIMO applications. The average antenna gain in the azimuthal plane for both the two antennas can meet the minimum average antenna gain required for practical applications of the internal WLAN antenna in the laptop computer [8–10]. Details of the proposed design are described.

2. PROPOSED DESIGN OF TWO ANTENNAS WITH IMPROVED ISOLATION

Figure 1 shows the geometry of two 2.4/5.2/5.8 GHz WLAN antennas with a dual-band strip resonator. The proposed design is easily printed on one surface of a thin FR4 substrate. In this study, a 0.8-mm thick FR4 substrate was used. The proposed design is mounted along the top edge of the large system ground plane of 260 × 200 mm^2, which can be considered as the supporting metal frame of the laptop display. Note that in the study, the proposed design is placed with a distance of 15 mm to the central line of the system ground plane, not at the central line. This arrangement considers the real case that the central region of the top edge of the system ground plane is usually reserved for the lens of the embedded digital camera in the laptop computer. There is also an antenna ground of 3 mm in height and 50 mm in length in the proposed design; through two connecting points C and C′, the antenna ground is electrically connected to

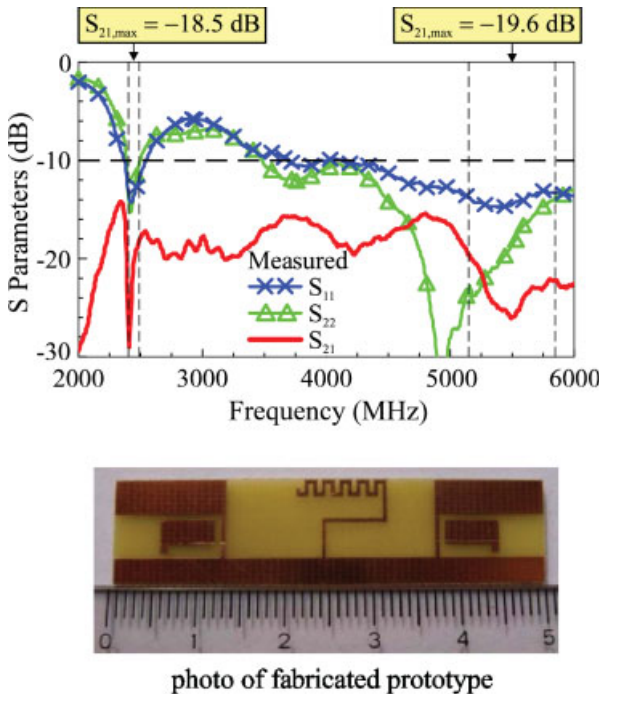

Figure 2 Measured S parameters and the photo of the fabricated prototype. [Color figure can be viewed in the online issue, which is available at www.interscience.wiley.com]

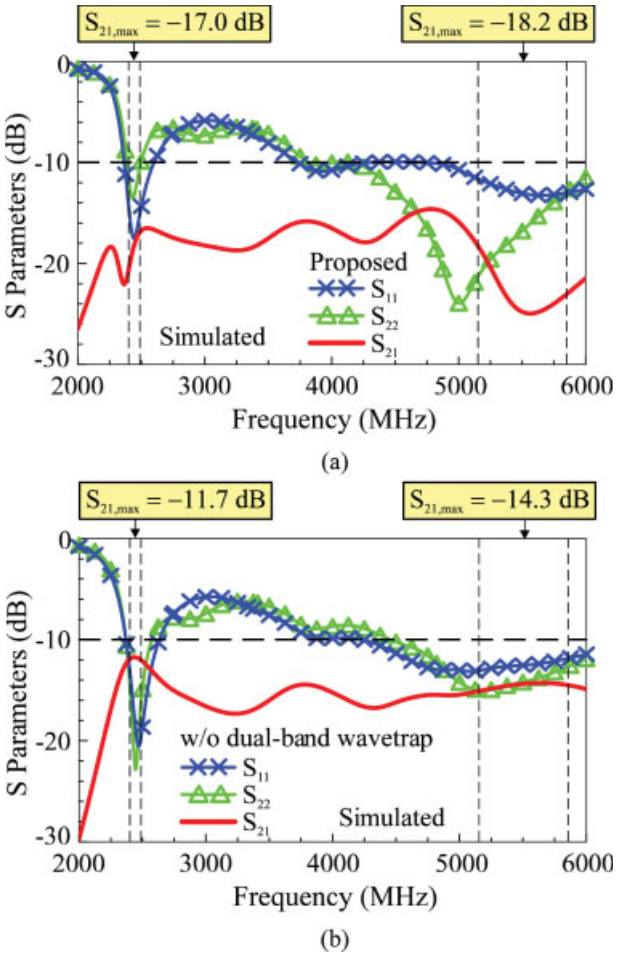

Figure 3 Simulated S parameters for (a) the proposed design and (b) the reference design (the corresponding design without the dual-band wavetrap). [Color figure can be viewed in the online issue, which is available at www.interscience.wiley.com]

the system ground plane. The length 50 mm is also considered as the total length (L) of the proposed design.

In addition to the antenna ground, the proposed design mainly comprises two small-size printed antennas capable of covering 2.4/5.2/5.8 GHz WLAN operation and a dual-band strip resonator as a wavetrap in-between the two antennas. When mounted along the top edge of the system ground plane, the proposed design shows a height of 9 mm and 50 mm in length. This required size along the top edge of the system ground plane is acceptable for practical laptop computer applications.

The two WLAN antennas are small-size uniplanar coupled-fed PIFA occupying same dimensions of 9×13 mm^2, whose detailed design considerations for a single element have been studied in [8]. Antenna 1 of the proposed design is treated as Port 1, at which a 50-Ω coaxial line is connected with its central conductor at point A and its outer grounding sheath at point B. Similarly, Antenna 2 is treated as Port 2 in the proposed design; a 50-Ω coaxial line is also used to feed the antenna, with its central conductor at point B′ and its outer grounding sheath at point B′. Antenna 1 and 2 are also arranged to have their shorting arms facing to each other, which can decrease the antenna's near-field radiation in-between the two antennas and lead to smaller mutual coupling [18, 19, 21]. However, with a spacing (d) of 24 mm between the two antennas mounted along the top edge of a large ground plane in this study, there is large mutual coupling between the two antennas [the S_{21} over the 2.4 GHz band can be as large as about −11.7 dB, see Fig. 3(b) in Section 3], which is not acceptable for practical applications. When the spacing d decreases (the total length $L = 26$ mm $+ d$ also decreases), the S_{21} will further increase to be larger than −10 dB; that is, the mutual coupling between the two antennas will be degraded further. For laptop computer applications, the S_{21} between the two antennas over the operating bands should be less than about −16 dB. In this case, with the inclusion of the long coaxial line (usually about 70 cm), which is estimated to cause the power loss of about −2 dB for frequencies over the 2.4 GHz band and about −4 dB over the 5.2/5.8 GHz bands, the S_{21} between the two antennas over the operating bands will be less than −20 dB, good for practical applications.

The embedded strip resonator in-between the two antennas as shown in the figure has a meandered end section, which is mainly used for adjusting its second resonance to occur at about 5.5 GHz, while keeping the first resonance at about 2.45 GHz. It is well known that the first two resonances of the linear straight strip monopole usually show a frequency ratio of about 1 to 3 [22, 23]. This also applies to the shorted strip resonator in the proposed design. By introducing the meandering in the strip's end section, the excited surface current distributions of the higher-order resonances of the strip resonator in the proposed

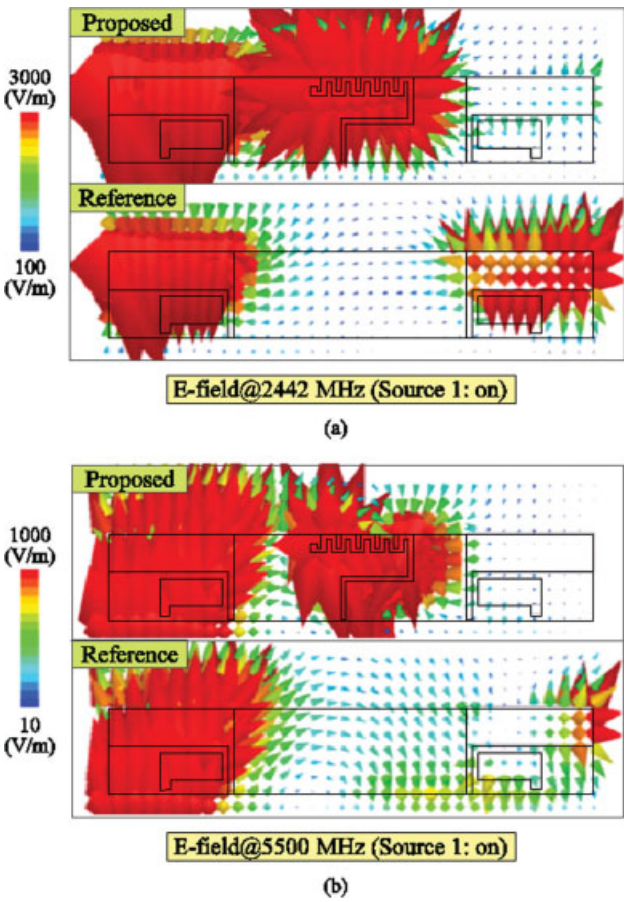

Figure 4 Simulated electric-field distribution evaluated at 1 mm above the metal portion of the proposed design and the reference design in Figure 3. (a) 2442 MHz. (b) 5500 MHz. [Color figure can be viewed in the online issue, which is available at www.interscience.wiley.com]

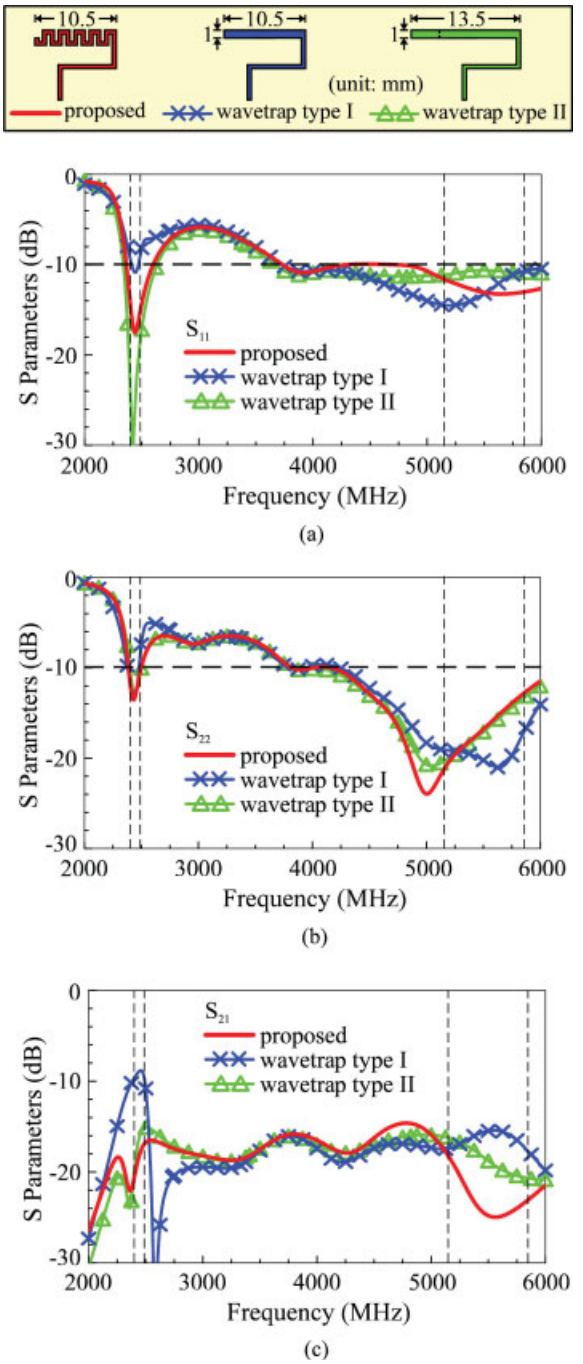

Figure 5 Simulated S parameters for the proposed design and the reference design with different strip resonators; dimensions of Antenna 1 and 2 are the same as given in Figure 1. (a) S_{11}. (b) S_{22}. (c) S_{21}. [Color figure can be viewed in the online issue, which is available at www.interscience.wiley.com]

design can be effectively modified, which can make the first two resonances of the embedded strip resonator occur at about the desired 2.45 and 5.5 GHz. In this case, the embedded strip resonator can function as an effective wavetrap to trap or block the antenna's near-field radiation from Antenna 1 to Antenna 2 or vice versa. This behavior results in decreased mutual coupling between the two antennas with a fixed spacing. More detailed functions of the embedded strip resonator will be discussed with the aid of Figures 4 and 5 in the next section.

3. RESULTS AND DISCUSSION

The proposed design was fabricated and tested. Figure 2 shows the measured S parameters of the proposed design. A photo of the fabricated prototype is also shown in the figure. Good impedance matching (S_{11} at Port 1 and S_{22} at Port 2 less than -10 dB) over the 2.4 and 5.2/5.8 GHz bands is seen for Antenna 1 and 2. The measured S_{21} seen at Port 2 with Port 1 (Antenna 1) excited is less than -18.5 dB over the 2.4 GHz band and -19.6 dB over the 5.2/5.8 GHz bands, which is acceptable for practical laptop computer applications.

Figure 3 shows the comparison of the simulated S parameters for the proposed design and the reference design (the corresponding design without the dual-band strip resonator or wavetrap). It is first seen that the simulated results obtained using Ansoft HFSS [24] shown in Figure 3(a) agree well with the measured data shown in Figure 2. For the results of the reference design shown in Figure 3(b), the simulated S_{21} is larger than those of the proposed design in Figure 3(a), especially for frequencies over the 2.4 GHz band (-11.7 vs. -17.0 dB). The presence of the dual-band strip resonator or wavetrap indeed decreases the mutual coupling between Antenna 1 and 2. Also notice that for both cases, good impedance matching with S_{11} and S_{22} less than -10 dB over the 2.4 and 5.2/5.8 GHz bands is seen in Figures 3(a) and 3(b).

Figure 4 shows the simulated electric-field distribution evaluated at 1 mm above the metal portion of the proposed design and the reference design in Figure 3. In Figure 4(a), the results at 2442 MHz are shown, while those at 5500 MHz are shown in Figure 4(b). It is clearly seen that for both cases of 2442 and 5500 MHz, the strip resonator functions as an effective wavetrap for trapping the near-field radiation of Antenna 1 from entering into Antenna 2. This can explain the improved isolation obtained for the proposed design with the presence of the dual-band strip resonator.

Effects of the proposed strip resonator are further analyzed. Figure 5 shows the simulated S parameters for the proposed design and the reference design with different strip resonators or wavetraps (see the inset in the figure). Two other strip

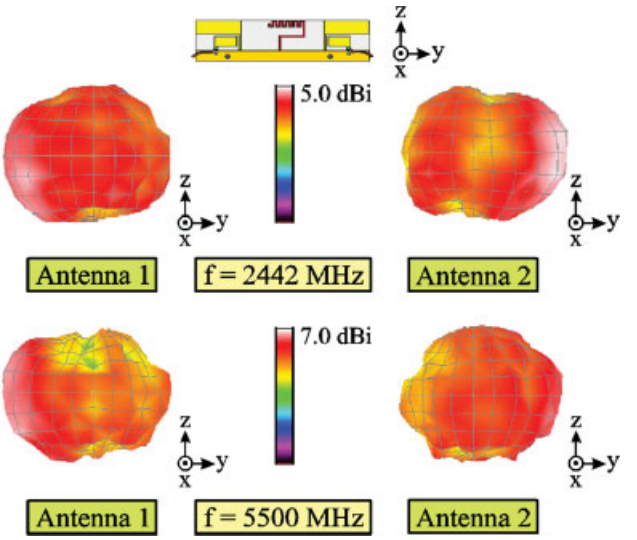

Figure 6 Measured 3D total-power radiation patterns for Antenna 1 and 2 at 2442 and 5500 MHz for the proposed design. [Color figure can be viewed in the online issue, which is available at www.interscience.wiley.com]

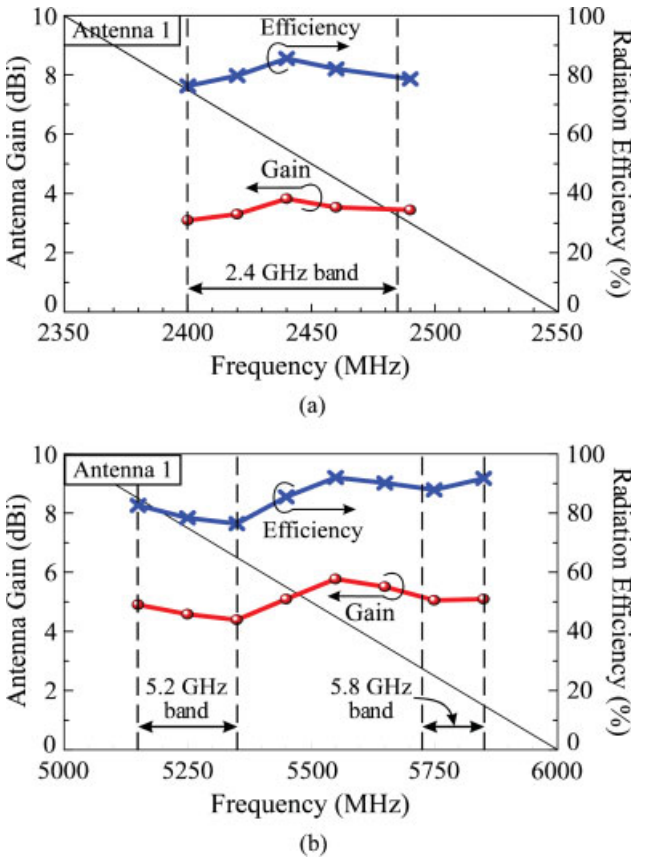

Figure 7 Measured antenna gain and radiation efficiency for Antenna 1 of the proposed design. (a) 2.4 GHz band. (b) 5.2/5.8 GHz bands. [Color figure can be viewed in the online issue, which is available at www.interscience.wiley.com]

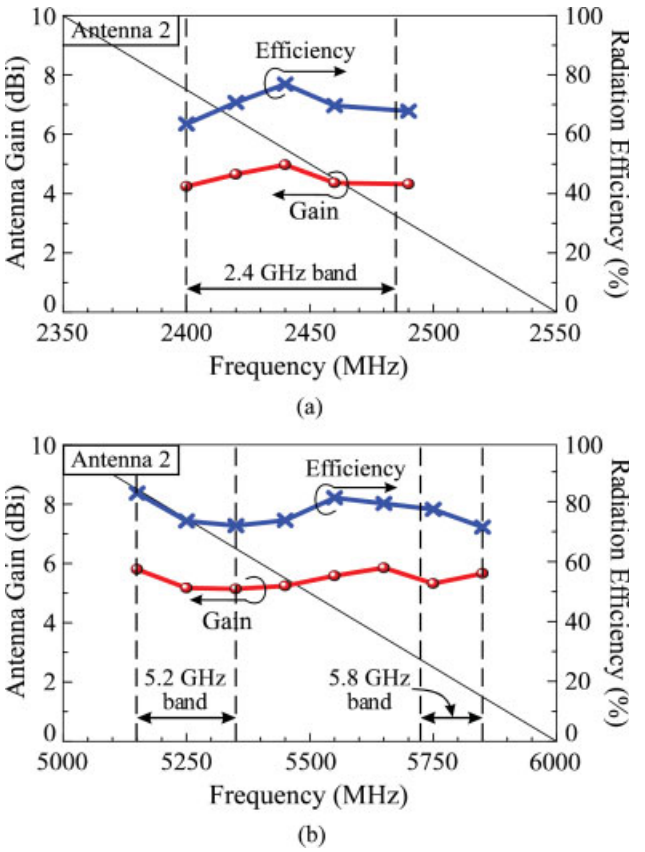

Figure 8 Measured antenna gain and radiation efficiency for Antenna 2 of the proposed design. (a) 2.4 GHz band. (b) 5.2/5.8 GHz bands. [Color figure can be viewed in the online issue, which is available at www.interscience.wiley.com]

resonators (wavetrap type I and II) different from the one applied in the proposed design in Figure 1 are analyzed. No meandering is introduced in the end sections of the wavetrap type I and II. The length of the wavetrap type I is about 27 mm, corresponding to about 0.25 wavelength at 2600 MHz, while the length of the wavetrap type II is about 30 mm, corresponding to about 0.25 wavelength at 2442 MHz. The dimensions of Antenna 1 and 2 are all the same for the three cases. In Figure 5(a) for S_{11} and Figure 5(b) for S_{22}, the impedance matching over the 2.4 and 5.2/5.8 GHz bands is seen to all better than -10 dB for the three cases, although there are some variations in the impedance matching for using different strip resonators. For S_{21} shown in Figure 5(c), it is first seen that over the 2.4 GHz band, the S_{21} for the wavetrap type I shows a high value of larger than -10 dB. This is mainly because the strip length of the wavetrap type I has a resonance (0.25 wavelength resonance) at about 2.6 GHz, not at about 2.45 GHz. While for the wavetrap type II, its end section is lengthened such that the total length of the wavetrap type II is increased to be about 30 mm, hence resulting in to a 0.25 wavelength resonance occurred at about 2.45 GHz. This leads to decreased S_{21} obtained over the 2.4 GHz band for the wavetrap type II. However, only for the proposed design in which the end section of the strip resonator is meandered such that the first two resonances of the strip resonator can be adjusted to occur at about 2.45 and 5.5 GHz to have good S_{21} obtained for both the desired 2.4 and 5.2/5.8 GHz bands. This explains the necessity in using the dual-band strip resonator shown in Figure 1 to achieve good isolation between Antenna 1 and 2.

Figure 6 shows the measured three-dimensional (3-D) total-power radiation patterns for Antenna 1 and 2 at 2442 and 5500 MHz for the proposed design. Some variations in the measured radiation patterns for the two antennas are seen. This is mainly owing to the different antenna locations and orientations at the

TABLE 1 Simulated Maximum S_{21} with and without the Wavetrap Over the 2.4 and 5.2/5.8 GHz Bands

	$S_{21,max}$ (dB) in 2.4 GHz Band			$S_{21,max}$ (dB) in 5.2/5.8 GHz Bands		
L,d (mm)	With Wavetrap	Without Wavetrap	Improvement in S_{21}	With Wavetrap	Without Wavetrap	Improvement in S_{21}
50, 24	−17.0	−11.7	5.3	−18.2	−14.3	3.9
48, 22	−15.9	−11.2	4.7	−18.9	−13.8	5.1
46, 20	−13.5	−10.6	2.9	−19.3	−14.0	5.3
44, 18	−11.3	−10.0	1.3	−21.4	−14.5	6.9
42, 16	−9.8	−9.3	0.5	−20.8	−15.0	5.8

The length L decreases with the decreasing distance d between the two antennas ($L = 26$ mm $+ d$); other dimensions are the same as given in Figure 1.

TABLE 2 Measured Average Antenna Gain in the Azimuthal Plane for Antenna 1 and 2 Shown in Figure 1

Average Antenna Gain (dBi)		Antenna 1 (dBi)	Antenna 2 (dBi)	Including 70-cm Coaxial-Line Loss		Specification (dBi)
				Antenna 1 (dBi)	Antenna 2 (dBi)	
2.4 GHz band	2400 MHz	−0.1	0.5	−2.1	−1.5	−4.0
	2442 MHz	0.1	0.7	−1.9	−1.3	−4.0
	2484 MHz	0.1	1.1	−1.9	−0.9	−4.0
5.2/5.8 GHz bands	5150 MHz	0.0	0.6	−4.0	−3.4	−5.0
	5350 MHz	0.5	0.2	−3.5	−3.8	−5.0
	5500 MHz	1.0	0.0	−3.0	−4.0	−5.0
	5725 MHz	1.2	0.2	−2.8	−3.8	−5.0
	5875 MHz	0.7	0.0	−3.3	−4.0	−5.0

The specification is the minimum average antenna gain required for practical applications of the internal WLAN antenna in the laptop computer [8–10].

top edge of the system ground plane. However, near omnidirectional direction is observed in the azimuthal plane (*x-y* plane) of the two antennas. Figure 7 shows the measured antenna gain and radiation efficiency for Antenna 1 of the proposed design. Over the 2.4 GHz band shown in Figure 7(a), the radiation efficiency is about 77–86% and the antenna gain is about 3.0–3.7 dBi. While the results over the 5.2/5.8 GHz bands are shown in Figure 7(b). The radiation efficiency is about 76–92% and the antenna gain is about 4.3–5.7 dBi. The corresponding results for Antenna 2 of the proposed design are presented in Figure 8. The results for Antenna 2 show some small variations compared to those for Antenna 1. Again, this is owing to the different antenna locations and orientations at the top edge of the system ground plane.

In the above study, the spacing d between the two antennas is fixed as 24 mm, and the total length L of the proposed design is 50 mm ($= 26$ mm $+ d$). Results for varying the spacing d are also studied, while the dimensions of Antenna 1 and 2 are fixed as given in Figure 1. The obtained simulated results for the maximum S_{21} over the 2.4 and 5.2/5.8 GHz bands are listed in Table 1 for comparison. The improvement in S_{21} over the 2.4 GHz band is decreased from 5.3 to 0.5 dB when the spacing d decreases from 24 to 16 mm. This indicates that when the spacing d is too small, the effects of the embedded strip resonator become limited. Conversely, the S_{21} can still be effectively improved over the 5.2/5.8 GHz bands even when the spacing d decreases. This behavior is largely because the wavelengths of the frequencies over the 5.2/5.8 GHz bands are much smaller than those over the 2.4 GHz band; hence, with a small spacing of d, the embedded strip resonator can still function as a good wavetrap or reflector over the 5.2/5.8 GHz band for blocking the near-field radiation from Antenna 1 to Antenna 2 or vice versa.

In addition to the radiation efficiency and antenna gain studied in Figures 7 and 8, the average antenna gain in the azimuthal plane of Antenna 1 and 2 is also an important factor considered for practical laptop computer applications [8–10]. The measured average antenna gain in the azimuthal plane is defined as the antenna gain over all of the ϕ angles. This factor is considered to ensure that there will be no large dips or nulls in the antenna's radiation patterns in the azimuthal plane such that good coverage in all directions of the azimuthal plane of the laptop computer will be obtained. The average antenna gain in the azimuthal plane for Antenna 1 and 2 is hence measured and listed in Table 2 for comparison. The required minimum value of the average antenna gain is also shown in the table [8–10]. Results for the condition including the power loss of the long coaxial line (usually about 70 cm) connected to the internal WLAN antenna in the laptop computer are also given in the table. As stated earlier, the power loss of the 70-cm-long coaxial line is estimated to be −2 dB for frequencies over the 2.4 GHz band and −4 dB over the 5.2/5.8 GHz bands. The obtained results indicate that the average antenna gain of Antenna 1 and 2 in the proposed design meets the specification for practical laptop computer applications.

4. CONCLUSION

Isolation improvement using an embedded dual-band strip resonator in-between two internal coupled-fed PIFAs for 2.4/5.2/5.8 GHz WLAN operation in the laptop computer has been demonstrated. The proposed design can be easily implemented on a thin FR4 substrate at low cost and is hence especially suitable for thin-profile laptop computer applications. The embedded strip resonator in-between the two antennas functions as a wavetrap over the 2.4 and 5.2/5.8 GHz bands to effectively reduce the mutual coupling between the two antennas through trapping or blocking the near-field radiation from one antenna to another. The proposed design with a reasonable size of 9×50 mm^2 along the top edge of the large system ground plane of the laptop computer can hence achieve good isolation over the two desired operating bands for 2.4/5.2/5.8 GHz WLAN operation. Further, good radiation characteristics of the two antennas have also been obtained. The measured average antenna gain in the azimuthal plane of the two antennas has been found to meet the requirements for practical applications of the internal WLAN antenna in the laptop computer.

REFERENCES

1. Wikipedia, the free encyclopedia, available at: http://en.wikipedia.org/wiki/Netbook.
2. D. Liu and B. Gaucher, A triband antenna for WLAN applications, IEEE Antennas and Propagation Society International Symposium Digest 2, Columbus, OH, 2003, pp. 18–21.
3. C.M. Su, W.S. Chen, Y.T. Cheng, and K.L. Wong, Shorted T-shaped monopole antenna for 2.4/5 GHz WLAN operation, Microwave Opt Technol Lett 41 (2004), 202–203.
4. K.L. Wong, L.C. Chou, and C.M. Su, Dual-band flat-plate antenna with a shorted parasitic element for laptop applications, IEEE Trans Antennas Propag 53 (2005), 539–544.
5. K.L. Wong and L.C. Chou, Internal composite monopole antenna for WLAN/WiMAX operation in the laptop computer, Microwave Opt Technol Lett 48 (2006), 868–871.
6. L.C. Chou and K.L. Wong, Uni-planar dual-band monopole antenna for 2.4/5 GHz WLAN operation in the laptop computer, IEEE Trans Antennas Propag 55 (2007), 3739–3741.
7. J. Yeo, Y.J. Lee, and R. Mittra, A novel dual-band WLAN antenna for notebook platforms, IEEE Antennas and Propagation Society International Symposium Digest 2, Monterey, CA, 2004, pp. 1439–1442.
8. C.T. Lee and K.L. Wong, Uniplanar printed coupled-fed PIFA with a band-notching slit for WLAN/WiMAX operation in the laptop computer, IEEE Trans Antennas Propag 57 (2009), 1252–1258.

9. S.J. Liao, K.L. Wong, and L.C. Chou, Small-size uniplanar coupled-fed PIFA for 2.4/5.2/5.8 GHz WLAN operation in the laptop computer, Microwave Opt Technol Lett 51 (2009), 1023–1028.
10. K.L. Wong and W.J. Chen, Small-size microstrip-coupled printed PIFA for 2.4/5.2/5.8 GHz WLAN operation in the laptop computer, Microwave Opt Technol Lett 51 (2009).
11. K.L. Wong, Planar antennas for wireless communications, Wiley, New York, 2003.
12. C.H. Chang and K.L. Wong, Internal coupled-fed shorted monopole antenna for GSM850/900/1800/1900/UMTS operation in the laptop computer, IEEE Trans Antennas Propag 56 (2008), 3600–3604.
13. K.L. Wong and L.C. Lee, Multiband printed monopole slot antenna for WWAN operation in the laptop computer, IEEE Trans Antennas Propag 57 (2009), 324–330.
14. K.L. Wong and S.J. Liao, Uniplanar coupled-fed printed PIFA for WWAN operation in the laptop computer, Microwave Opt Technol Lett 51 (2009), 549–554.
15. K.L. Wong and F.H. Chu, Internal planar WWAN laptop computer antenna using monopole slot elements, Microwave Opt Technol Lett 51 (2009), 1274–1279.
16. K.L. Wong, C.H. Chang, B. Chen, and S. Yang, Three-antenna MIMO system for WLAN operation in a PDA phone, Microwave Opt Technol Lett 48 (2006), 1238–1242.
17. G. Chi, B. Li, and D. Qi, Dual-band printed diversity antenna for 2.4/5.2-GHz WLAN application, Microwave Opt Technol Lett 45 (2005), 561–563.
18. K.J. Kim and W.H. Ahn, The high isolation dual-band inverted F antenna diversity system with the small N-section resonators on the ground plane, Microwave Opt Technol Lett 49 (2007), 731–734.
19. M. Karaboikis, C. Soras, G. Tsachtsiris, and V. Makios, Compact dual-printed inverted-F antenna diversity systems for portable wireless devices, IEEE Antennas Wireless Propag 3 (2004), 9–14.
20. Y. Gao, C.C. Chiau, X. Chen, and C.G. Parini, Modified PIFA and its array for MIMO terminals, IEE Proc Microwave Antennas Propag 152 (2005), 255–259.
21. K.L. Wong, Y.Y. Chen, S.W. Su, and Y.L. Kuo, Diversity dual-band planar inverted-F antenna for WLAN operation, Microwave Opt Technol Lett 38 (2003), 223–225.
22. C.T. Lee, K.L. Wong, and Y.C. Lin, Wideband monopole antenna for DTV/GSM operation in the mobile phone, Microwave Opt Technol Lett 50 (2008), 801–806.
23. T.W. Kang and K.L. Wong, Chip-inductor-embedded small-size printed strip monopole for WWAN operation in the mobile phone, Microwave Opt Technol Lett 51 (2009), 966–971.
24. Ansoft Corporation HFSS, available at:http://www.ansoft.com/products/hf/hfss/.

NANOELECTROMECHANICAL SWITCHES FOR RECONFIGURABLE ANTENNAS

Bedri A. Cetiner,[1] Necmi Biyikli,[2] Bahadir S. Yildirim,[3] and Yasin Damgaci[1]
[1] Department of Electrical and Computer Engineering, Utah State University, Logan, UT 84341; Corresponding author: bedri@engineering.usu.edu
[2] UNAM—Institute of Materials Science and Nanotechnology, Bilkent University, Bilkent, Ankara 06800, Turkey
[3] MEMSComm LLC, KY 40351

Received 24 April 2009

ABSTRACT: *We report on the full-wave analyses of a frequency reconfigurable antenna integrated with metallic nanoelectromechanical system (NEMS) switches (length = 3 μm, width = 60 nm). The NEMS switch used in this work has the same architecture with low voltage, double-arm cantilever-type metallic DC-contact microelectromechanical system (MEMS) switch recently developed in author's group. The microfabrication and characterization of the MEMS switch have also been given in this article.* © 2009 Wiley Periodicals, Inc. Microwave Opt Technol Lett 52: 64–69, 2010; Published online in Wiley InterScience (www.interscience.wiley.com). DOI 10.1002/mop.24833

Key words: *multifunctional reconfigurable antenna; microelectromechanical system (MEMS) switch; nanoelectromechanical system (NEMS) switch; full-wave electromagnetic analysis*

1. INTRODUCTION

The multifunctional reconfigurable antenna (MRA) concept [1] has gained significant interest due to the following two main factors: (A) A single MRA that can perform multiple functions by dynamically changing its properties (operating frequency, polarization, radiation pattern, etc) can replace multiple single-function legacy antennas, thereby providing a significant reduction in the overall size of multimode multiband wireless communication systems. (B) Reconfigurable antenna properties of an MRA can be used as important additional degrees of freedom in adaptive system parameters as first proposed in Ref. [2], which was further studied [3].

To dynamically change the properties of an MRA, the current distribution over the volume of the antenna needs to be changed, where each distribution corresponds to a different mode of operation. To this end, one can change the geometry of the antenna by switching on and off various geometrical metallic segments that make up the MRA. For switching, microelectromechanical system (MEMS), nanoelectromechanical system (NEMS) or semiconductor type switches can be employed. MEMS and NEMS type switches are advantageous over semiconductor type switches mainly due to the monolithic integration capability with antenna segments, which eliminates interconnect losses, along with their very low loss and power characteristics [4]. However, standard MEMS switches require high actuation voltages (30–80 V) and posses low switching speeds (10–20 μs), which may not be appropriate for next generation cognitive wireless communications applications. In these systems, the reconfigurability must be fast enough (~less than 1 μs) to respond to short term channel statistics and to support most dynamic adaptation schemes such as opportunistic beamforming schemes. We have recently developed a double-arm DC-contact small-size MEMS switch [5] of which schematic and SEM picture are shown in Figure 1. Due to its small-size, cantilever length (L = 5–50 μm) and width (W = 2–40 μm), i.e., ~10–100 times smaller in lateral dimensions than a standard MEMS switch, this switch showed actuation voltages lower than 10 V. We have chosen DC-contact switches over their capacitive contact counterparts due to their wide frequency range of operation, which is compatible with IEEE 802.11 WLAN standards.

The article is organized as follows: first, we briefly present the microfabrication and RF characterization of the reduced-size MEMS switches. Next, the full-wave analyses of a frequency reconfigurable antenna integrated with NEMS switches are given. This antenna, namely NEMS integrated penta-band PIFA can operate over five frequency bands of GSM900, GPS1575, GSM1800, PCS1900, and UMTS2100.

2. REDUCED-SIZE MEMS SWITCH: MICROFABRICATION AND RF CHARACTERIZATION

2.1. Microfabrication

The double-arm MEMS actuators were fabricated on a synthetic quartz substrate using a six-layer microwave compatible